

# Periodic orbits for three particles with finite angular momentum

Michael Nauenberg

Department of Physics

University of California, Santa Cruz, CA 95064

(Sept. 2001)

New solutions are obtained for the planar motion of three equal mass particles on a common periodic orbit with finite total angular momentum, under the action of attractive pairwise forces of the form  $1/r^{p+1}$ . It is shown that for  $-2 < p \leq 0$ , Lagrange's 1772 circular solution is the limiting case of a complex symmetric orbit. The evolution of this orbit and another recently discovered one in the shape of a figure eight is investigated for a range of angular momenta by a novel numerical method. Extensions to  $n$  equal mass particles and to three particles of different masses are also discussed briefly.

keywords: nonlinear science, orbital dynamics

## Introduction

Recently C. Moore<sup>1</sup> applied the theory of braids to find a classification of periodic orbits for the motion of several particles moving in a plane under the action of pairwise attractive power-law forces, obtaining numerical results for the case of 2 and 3 strands. In particular, for three particles of equal mass, he found a solution where these particles travel on a common orbit in the shape of a figure eight. This orbit was found also independently by A. Chenciner and R. Montgomery<sup>2,3</sup> who have proved its existence for the case of zero total angular momentum and inverse square forces. Moore's numerical result that this orbit is stable has also been confirmed by computations of C Simó<sup>4</sup>. Previously, one of the simplest known periodic orbits without collisions for this problem<sup>5</sup> was Lagrange's classic solution<sup>6</sup> where the three particles form the vertices of an equilateral triangle with each particle moving on an elliptic orbit with focus in the common center of mass. In this paper we show that for attractive power-law forces of the form  $1/r^{p+1}$  with  $-2 < p \leq 0$ , the circular Lagrange orbit is the limit of a family of orbits which are periodic in a uniformly rotating frame of reference. For small deviations, we find analytically that this orbit is a distorted ellipse which, as the angular momentum decreases, resembles a distorted figure eight shape, but it does not approach the recently discovered zero-angular-momentum figure eight orbit which has a different winding number. For this figure eight orbit, which exists for  $-2 < p$ , we obtain an analytic approximation, and we prove by perturbation theory that it can be extended to finite angular momentum. We also investigate the evolution of these two orbits for a finite range of total angular momentum by a novel iterative method, and consider briefly the case of such periodic orbits for  $n$  equal mass particles, and for three particles of different masses.

## Computational method for periodic orbits

Our method is based on expanding in a Fourier series the Cartesian coordinates for the periodic orbit on which all the three equal mass particles travel, and then finding the extremum of the action for this system with respect to the Fourier coefficients in a frame rotating with a fixed frequency  $\Omega$ . We obtain analytic approximations by perturbation theory, and numerical solutions by a novel iterative method which converges rapidly. Setting  $\theta = \omega t$ , where  $t$  is the time,  $\omega = 2\pi/\tau$  is the frequency, and  $\tau$  is the period of the orbit), we have

$$x(\theta) = \sum_{k=1}^{k=n} a_s(k_o) \sin(k_o \theta) + a_c(k_e) \cos(k_e \theta) \quad (1)$$

and

$$y(\theta) = \sum_{k=1}^{k=n} b_s(k_e) \sin(k_e \theta) + b_c(k_o) \cos(k_o \theta), \quad (2)$$

where  $k_o = 2k - 1$  and  $k_e = 2k$ , excluding multiples of the integer 3. In practice, the number of terms  $n$  in the Fourier sums, Eqs. 1 and 2, depends on the desired accuracy of the solution. The Cartesian coordinates of each of the three particles is then given by  $x_i = x(\theta_i)$  and  $y_i = y(\theta_i)$ , for  $i = 1, 2, 3$ , and the invariance of the action under the cyclic transformation  $1 \rightarrow 2 \rightarrow 3 \rightarrow 1$  is satisfied by the requirement  $\theta_1 = \theta$ ,  $\theta_2 = \theta + 2\pi/3$  and  $\theta_3 = \theta + 4\pi/3$ . These conditions are satisfied by the equations which determine the extremum of the action in a frame rotating with frequency  $\Omega$  in the plane of the orbit<sup>7</sup> which takes the form

$$A = \int_0^{2\pi} d\theta [K(\theta) - P(\theta) + \frac{1}{2} \Omega^2 I(\theta) + \Omega L(\theta)], \quad (3)$$

where  $K(\theta)$  is the kinetic energy,  $P(\theta)$  the potential energy,  $I(\theta)$  the moment of inertia, and  $L(\theta)$  the angular momentum in the rotating frame. These are given by the following expressions:

$$K(\theta) = \frac{1}{2}\omega^2 \sum_{i=1}^{i=3} \left(\frac{dx_i}{d\theta}\right)^2 + \left(\frac{dy_i}{d\theta}\right)^2, \quad (4)$$

$$P(\theta) = -\left(\frac{1}{p}\right)\left(\frac{1}{r_{12}^p} + \frac{1}{r_{13}^p} + \frac{1}{r_{23}^p}\right), \quad (5)$$

$$I(\theta) = \sum_{i=1}^{i=3} x_i^2 + y_i^2, \quad (6)$$

and

$$L(\theta) = \omega \sum_{i=1}^{i=3} x_i \frac{dy_i}{d\theta} - y_i \frac{dx_i}{d\theta}, \quad (7)$$

where  $r_{ij} = \sqrt{(x_i - x_j)^2 + (y_i - y_j)^2}$  is the distance between particles  $i$  and  $j$ , and  $p$  is the power of the force law,

The extrema of the action, Eq. 3, are obtained by finding the Fourier coefficients for which the partial derivatives of the action with respect to these coefficients vanish,

$$\frac{\partial A}{\partial a_s(k_o)} = u(k_o)a_s(k_o) - f_s(k_o) - v(k_o)b_c(k_o) = 0, \quad (8)$$

$$\frac{\partial A}{\partial b_c(k_o)} = u(k_o)b_c(k_o) - g_c(k_o) - v(k_o)a_s(k_o) = 0, \quad (9)$$

$$\frac{\partial A}{\partial b_s(k_e)} = u(k_o)b_s(k_e) - g_s(k_e) + v(k_o)a_c(k_e) = 0, \quad (10)$$

$$\frac{\partial A}{\partial a_c(k_e)} = u(k_o)a_c(k_e) - f_c(k_e) + v(k_o)b_s(k_e) = 0, \quad (11)$$

where  $u(k) = k^2\omega^2 + \Omega^2$  and  $v(k) = 2k\omega\Omega$ . Here the functions

$$f_s(k_o) = \frac{1}{\pi} \int_0^{2\pi} d\theta \frac{\partial P}{\partial x_1} \sin(k_o\theta), \quad (12)$$

$$f_c(k_e) = \frac{1}{\pi} \int_0^{2\pi} d\theta \frac{\partial P}{\partial x_1} \cos(k_e\theta), \quad (13)$$

$$g_s(k_e) = \frac{1}{\pi} \int_0^{2\pi} d\theta \frac{\partial P}{\partial y_1} \sin(k_e\theta), \quad (14)$$

$$g_c(k_o) = \frac{1}{\pi} \int_0^{2\pi} d\theta \frac{\partial P}{\partial y_1} \cos(k_o\theta). \quad (15)$$

depend also on all the Fourier coefficients.

We obtain numerical solutions of these equations by starting with the Fourier coefficients to some conjectured approximate period orbit, e.g. according to Moore's classification<sup>1</sup>, and then evaluating the partial derivatives of the action, Eqs. 8-11. If the extrema of the action is at a maximum (minimum), an improved orbit is then obtained by changing each coefficient in proportion to plus(minus) the corresponding partial derivative of the action. Thus, starting with some initial value for the coefficient  $a_s(k_o)$ , we obtain a new value  $a_s(k_o)$  by the relation

$$a'_s(k_o) = a_s(k_o) + \frac{\delta s}{u(k_o)} \frac{\partial A}{\partial a_s(k_o)} \quad (16)$$

with similar expressions for the other Fourier coefficients where  $\delta s$  is a positive (negative) parameter if the action is a maximum (minimum). This procedure is then iterated until the partial derivatives of the action are sufficiently small to any desired accuracy. Our method differs in an essential way from the standard method of steepest descent by the important factor  $1/u(k)$  which is essential for the convergence of the iterations with moderate values of  $\delta s$  (order .1).

To obtain analytic approximations of Eqs. 8-11, it is convenient to determine the frequencies  $\omega$  and  $\Omega$  by fixing the values of  $a_s(1)$  and  $b_c(1)$ , which give the scale of the orbit and the magnitude of the total angular momentum in the rest frame,  $L_t = L + \Omega I$ , where  $L$  is the mean angular momentum in the rotating frame, Eq. 7,

$$L = 3\omega \sum_{k=1}^{k=n} -k_o a_s(k_o) b_c(k_o) + k_e a_c(k_e) b_s(k_e), \quad (17)$$

and  $I$  is the mean moment of inertia, Eq. 6,

$$I = \frac{3}{2} \sum_{k=1}^{k=n} a_s(k_o)^2 + a_c(k_e)^2 + b_s(k_e)^2 + b_c(k_o)^2. \quad (18)$$

We have

$$\omega = \frac{1}{2}(\sqrt{\alpha} + \sqrt{\beta}) \quad (19)$$

and

$$\Omega = \frac{1}{2}(\sqrt{\alpha} - \sqrt{\beta}), \quad (20)$$

where

$$\alpha = \frac{f_s(1) - g_c(1)}{(1 - b_c(1))} \quad (21)$$

and

$$\beta = \frac{f_s(1) + g_c(1)}{(1 + b_c(1))} \quad (22)$$

are obtained from Eqs. 8 and 9 for  $k_o = 1$  and  $a_s(1) = 1$ . These frequencies scale with the size  $s$  of the orbit

according to the generalized Kepler relations that  $\omega^2 s^{p+2}$  and  $\Omega^2 s^{p+2}$  are constants.

The generalization of Lagrange's solution<sup>6</sup> is obtained by setting the Fourier coefficients  $a_c(k_e)$  and  $b_s(k_e)$  equal to zero, which according to Eqs. 11 and 10 implies that  $f_c(k_e)$  and  $g_s(k_e)$  also vanish. Small deviations from Lagrange's circular solution can be obtained by setting  $a_s(1) = 1$  and  $b_c(1) = 1 - \delta$ , and expanding Eqs. 8 and 9 in a power series  $\delta$ . In the limit of vanishing  $\delta$

$$\alpha = \frac{1}{3^{p/4}} \sqrt{-p/2} \quad (23)$$

which shows that these solutions exist only for  $p \leq 0$ . In particular, for the special case that  $p = -2$  corresponding to harmonic forces,  $\omega = \sqrt{3}$ ,  $\Omega = 0$ , and all the Fourier coefficients  $a_s(k_0)$  and  $b_c(k_0)$  vanish for  $k_0 > 1$ .

### Numerical solutions and analytic approximations

Two numerical solutions of the extended Lagrange problem are shown in Figs. 1 and 2, where segments of the orbit occupied by each particle during a third of a period are indicated by a dark line, a dotted line and a dashed line respectively, and ten successive locations on these segments are marked at equal intervals of time to illustrate the relative position and variable speed of the three particles moving on this orbit. In this solution the angular momentum of the orbit decreases as  $b_c(1)$  decreases, and the approximate elliptical orbit starts to get pinched in the middle. This is shown in Fig.1 for  $p = -.05$  at the special value  $b_c(1) = .049$  where the orbit also develops cusps at the two ends. At these values of the parameters each particle comes momentarily to rest at these points because the attractive forces due to the other two particles balance the centrifugal force in the rotating frame.

Further decrease of the value of  $b_c(1)$ , corresponding to decreasing angular momentum, requires that the y-component of velocity at these ends change direction, which is possible only if an additional lobe appears at each end. A further decrease of  $b_c(1)$  leads to an additional lobe at the center, as shown in Fig. 2 for  $p = -.05$  and  $b_c(1) = .0171$ .

The recently discovered<sup>1-3</sup> zero angular momentum periodic orbit in the shape of a figure eight is a solution of Eqs. 8 and 10 with the Fourier coefficients  $a_c(k_e)$  and  $b_c(k_o)$  set equal to zero. According to Eqs. 11 and 9, this implies that  $f_c(k_e) = g_c(k_o) = 0$ . For the special case that  $p = 2$ , it can be shown that the moment of inertia, Eq. 6, is a constant. Consequently the shape of this orbit can be determined from purely geometrical considerations by imposing the condition that the Fourier coefficients of an expansion of this moment and that of the angular momentum vanish. Keeping terms in the sums in Eqs. 1 and 2 up to  $n=4$ , we obtain

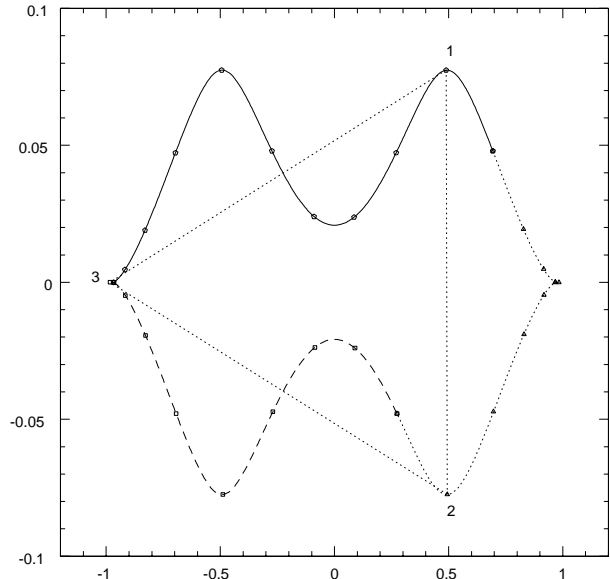


FIG. 1. An extension of Lagrange's circular orbit for three equal mass particles labeled here 1,2 and 3 , showing their location at ten equal time intervals during one third of a period. For example, when particle 3 reaches an extremum along the x-coordinate, its y-component of acceleration vanishes by symmetry, and therefore the location of the other two particles, 1 and 2, lie on the vertices of an isosceles triangle as shown here for the case  $p = -.05$  and  $b_c(1) = .049$ .

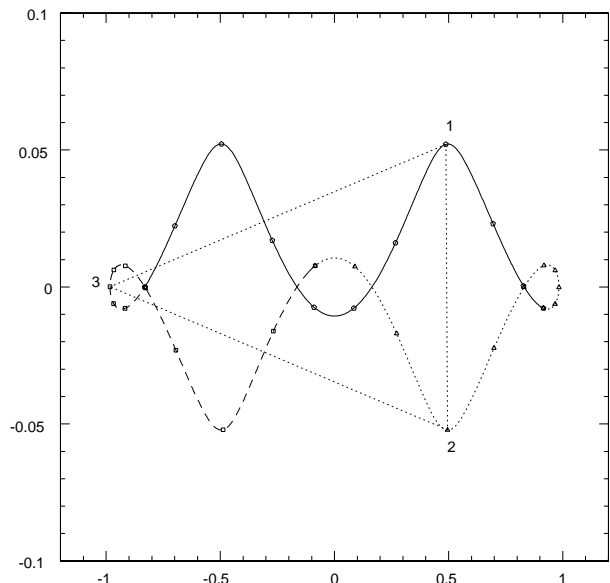


FIG. 2. Extended Lagrange orbit with crossings near the center and additional lobes at the two ends, for  $p = -.05$  and  $b_c(1) = .0171$

$$b_s(4) = \frac{b}{d} - \frac{b^3}{2d^4}(46 + 97b^2 + 49b^4), \quad (24)$$

$$a_s(5) = -\frac{b^2}{d} - \frac{b^2}{2d^4}(25 + 49b^2 + 22b^4), \quad (25)$$

$$a_s(7) = -\frac{b^2}{2d^2}, \quad (26)$$

$$b_s(8) = -\frac{b^3}{2d^2}, \quad (27)$$

where  $b = b_s(2)$  and  $d = 5 + 7b^2$ . The magnitude of  $b$  is determined by setting  $\omega = \sqrt{f_s(1)}$ , Eq. 19, and solving Eq. 10 for  $k_e = 2$  which takes the form  $b = h(b)$ , where

$$h(b) = \frac{g_s(2)}{4f_s(1)}. \quad (28)$$

We find that  $h(b)$  is a positive monotonically decreasing function for  $b > 0$  which diverges as  $b$  approaches zero, and vanishes as  $b$  increases indefinitely. Therefore, there exists only a single solution which we find at  $b = .3793$  corresponding to  $\omega = 1.448$ . This result is in good agreement with our numerical solution of Eqs. 8 and 10, which gives  $b = .3776$  and  $\omega = 1.452$ . The resulting figure eight orbit obtained from the Fourier coefficients given by Eqs. 24 - 28 is shown in Fig. 3, which is graphically indistinguishable from the orbit obtained from the numerical solution of Eqs. 8 and 10. Surprisingly, these analytic coefficients also give a good approximation to the zero-angular-momentum figure eight orbit for  $p < 2$ , because it turns out that the moment of inertia is approximately constant in this case<sup>4</sup>. As  $p$  decreases we find that  $b$  decreases and vanishes when  $p = -2$ , because in this limit of a harmonic force law the figure eight orbit becomes a linear collision orbit.

The zero-angular-momentum orbit provides the basis for a perturbation calculation of the corresponding orbit for small values of the angular momentum. Expanding the coefficients  $a_c(k_e)$  and  $b_c(k_o)$  in powers of  $b_c(1) = b$ , these coefficients together with the unperturbed coefficients  $a_s(k_o)$  and  $b_s(k_e)$  determine the angular momentum of the orbit. For example, for  $p = 1$  we find that  $\Omega = 1.647b$ , and substituting this value of  $\Omega$  and the lowest order Fourier coefficients in Eqs. 17 and 18 we obtain  $L_t = -.5276b$ . Solutions for larger values of  $b$  are obtained numerically by iterating these equations, fixing  $a_s(1)$  and starting with some arbitrary value for  $b_s(2)$ , while all other Fourier coefficients are initially set equal to zero. As  $b$  increases the figure eight orbit becomes more asymmetric with respect to the y-axis, as expected from the increasing action of the centrifugal and Coriolis forces in the rotating frame of reference, and at a critical value of the angular momentum the y-component of the velocity of the particle at the end of the orbit in a direction opposite to the rotation vanishes giving rise to a

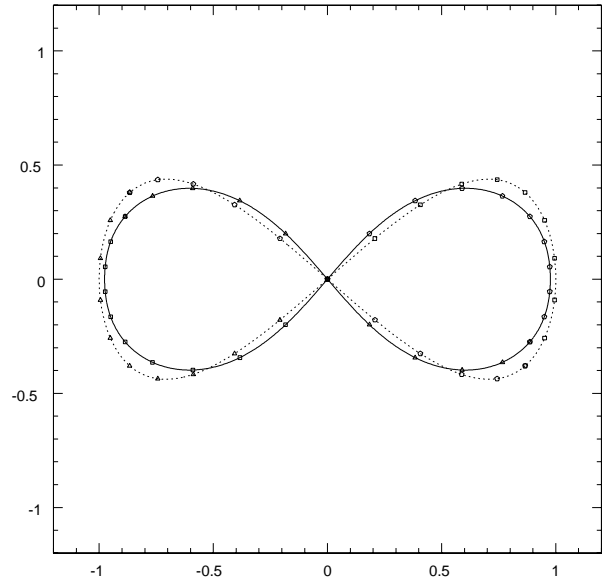


FIG. 3. Two analytic approximations to the figure eight periodic orbit with zero angular momentum for  $p = 2$ . The dashed line is the solution for  $n=1$ , a lemniscate, and the solid line is the solution given by Eqs. 23-26 for  $n=4$

cusp. A further increase of the angular momentum then requires that this component of velocity change sign at this point, which give rise to an additional loop in the orbit, as shown in Fig. 4.

Finite angular momentum solutions can also be obtained by rotating the figure eight orbit about an axis in the plane of the original orbit leading to a three dimensional orbit as shown in Fig. 5

Solutions of our equations provide initial conditions for a numerical integration of the equations of motion which can then be applied to study the stability of these periodic orbits with respect to small perturbations. A preliminary investigation indicates that some of these solutions are stable over a restricted range of angular momentum and values of  $p^8$ . Our method can readily be extended to investigate similar periodic motions for an arbitrary number of equal mass particles moving on the same orbit, many of which have been discovered recently<sup>9</sup>. For example, any odd number  $n_o$  of particles can travel on a figure eight orbit similar to that shown in Fig. 3. We find that this orbit, Fig. 6, approaches a unique limit as  $n_o \rightarrow \infty$ , but the frequency increases logarithmically with  $n_o$ .

In contrast, for the extension of Lagrange's circular orbit each additional particle leads to a different orbital curve. Finally we have also applied our method to study the case of three particles with different masses which must move, however, along different orbital curves. An example is shown in Fig. 7 which is an extension of an

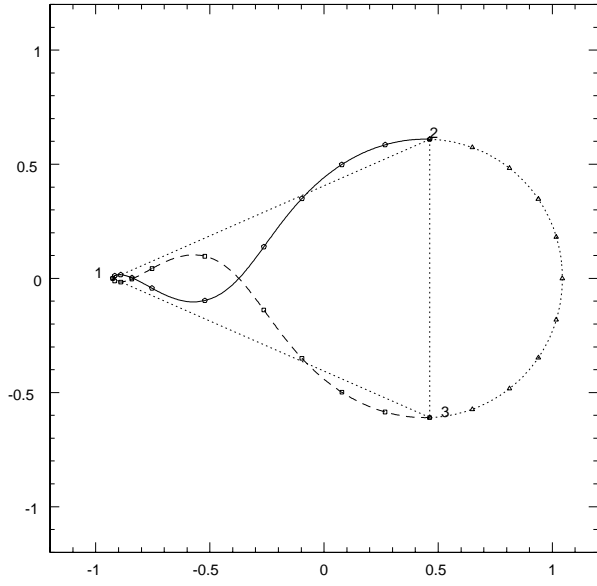


FIG. 4. Asymmetric figure eight periodic orbit with finite angular momentum in a rotating frame for  $p = 1$  and  $b = .38$ . The additional loop shown at the left end of the orbit forms when  $b > .34$ .

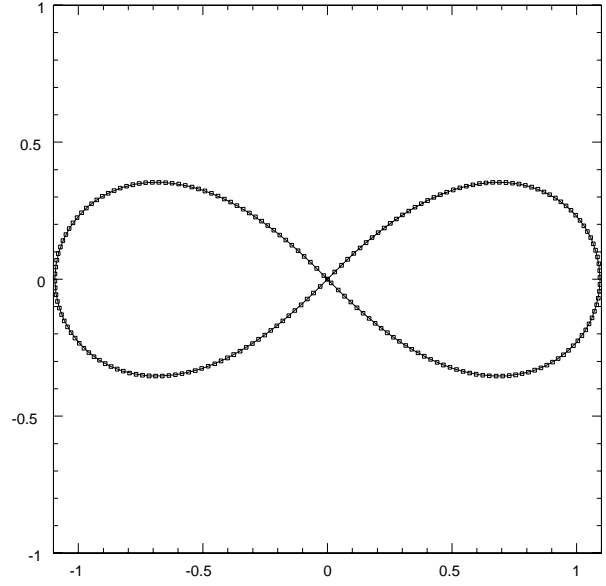


FIG. 6. Figure eight orbit with 201 particles

orbit discovered by Moore<sup>1</sup> for the case of equal mass particles.

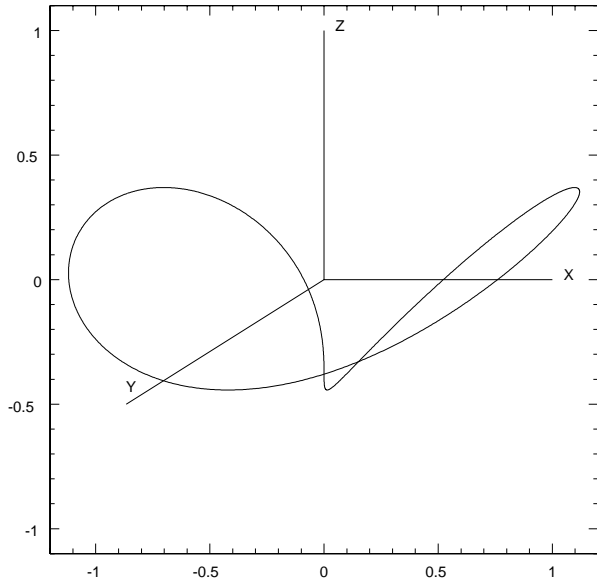


FIG. 5. Three dimensional figure eight orbit with finite angular momentum along the z-axis.

## Acknowledgements

I would like to thank Richard Montgomery for stimulating my interest in this problem and for many useful discussions, and Alan Chenciner and Charles Simó for helpful comments.

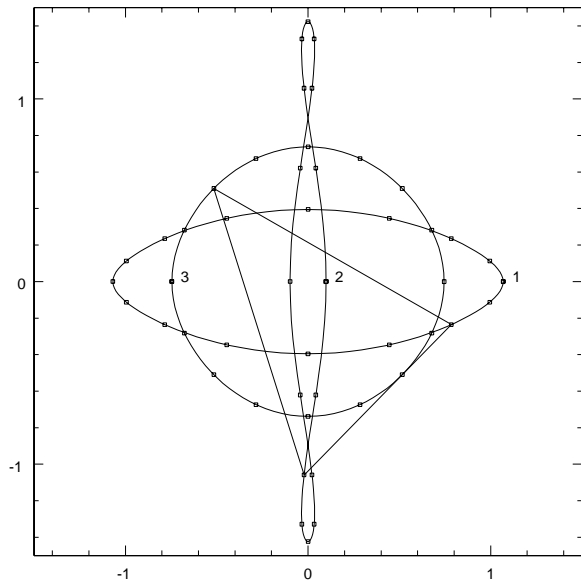


FIG. 7. Periodic orbits for three particles with masses 1.0, .5 and 1.5 at initial positions labeled 1, 2, and 3 respectively, under the action of inverse square pairwise forces. Particles 1 and 2 move initially clockwise, while particle 3 moves anti-clockwise. Positions are shown at  $1/16$  of a period, and the vertex of the triangle shows their relative position after  $1/8$  of a period.

- 
- <sup>1</sup> C. Moore, Phys. Rev. Lett. 70 (1993) 3675.  
<sup>2</sup> A. Chenciner and R. Montgomery, Annals of Mathematics 152 (2000) 881.  
<sup>3</sup> R. Montgomery, Notices of the American Mathematical Society (May, 2001) 471.  
<sup>4</sup> C. Simó, *Dynamical properties of the eight solution of the three-body problem*, to appear in the Proceedings of a Chicago conference dedicated to Don Saari (December 15-19, 1999). The numerical calculations in this paper are an order of magnitude more precise than those of C. Moore, ref. 1, who used steepest descent on discretized orbits.  
<sup>5</sup> Newton obtained the first periodic orbit for a three-body system in his treatment of the lunar problem, *Principia*, Book 3, Prop. 28. His solution was later derived more fully by L. Euler and by G.W. Hill.  
<sup>6</sup> J.L. Lagrange, *Essai sur le Problème des Trois Corps*, Oeuvres (Paris 1873) Vol. 6, pp. 272-292. Lagrange's solution can be readily extended to  $n$  bodies on the vertices of an  $n$ -polygon.  
<sup>7</sup> Similar relations apply for rotation along any other direction.  
<sup>8</sup> According to the virial theorem, for  $p \geq 2$  all orbits are unstable because the total energy  $E \geq 0$ .  
<sup>9</sup> A. Chenciner, J. Gerver, R. Montgomery and C. Simó, *Simple Choreographic Motions of  $N$  Bodies: A preliminary Study*, (Montgomery, private communication)